Trends on Noise Parameters Measurement for High Frequency Devices and their Modelling

Daniel Pasquet, Philippe Descamps, Dominique Lesénéchal

Abstract – **In this paper, we present the conventional noise parameters measurement methods that use a complicate and expensive set-up. They use a noise receiver, an impedance tuner, a calibrated noise source and a vector network analyzer. All this is controlled by heavy software. We show a more synthetic representation of the noise leading to a new measurement process where no impedance tuner is used. At the end, we detail how a transistor (an HBT) can be simply characterized by simple correlation matrices transformation. Then, we give some perspectives toward a method using only a modern vector network analyzer without receiver, noise source nor tuner.**

Keywords – **noise parameters, noise measurement, microwave, HBT noise model.**

I. Introduction

In modern mobile communication technologies, several targets are aimed in the context of sustainable development: the energy consumption from batteries and mains, the radiation into the user's body, the number of base stations. All these points strongly depend upon the sensitivity of the amplifier that is placed at the input of a reception chain. The sensitivity is represented by the ability to discriminate the signal from the noise. It is important to refine the noise figure of the input amplifier. This is reached by optimizing the environment of the first stage transistor of the amplifier. It is possible only if the transistor noise characteristics are well known. This implies that an efficient measurement process allows accurately reach the component characteristics [1].

II. General context

A hertzian transmission quality, with a digital modulation (Fig. 2), is characterized by the bit error rate (BER) during the demodulation and the data restitution.

Several quality classes exist. They are defined by international bodies. Error correcting codes also exist. They improve the transmission quality of a very noisy transmission channel [2]. None less, the transmission quality is generally considered as strongly degraded and makes the link unavailable when the bit error rate is greater than 10^{-3}. The link becomes unavailable in particular because of the synchronization bits loss.

The BET depends upon the ratio between the carrier and the noise (quoted as *C/N*) at the amplifier input but also on the

Daniel Pasquet, Philippe Descamps and Dominique Lesénéchal are with LaMIPS laboratory, 6 boulevard du Maréchal Juin, 14050 Caen, France, d.pasquet@ieee.org

modulation nature (Fig. 1) [3]. The power of the carrier is given by Eq. 1:

$$P_D = P_E G_1 G_2 \left(\frac{\lambda}{4\pi d}\right)^2 G_R \frac{1}{A_s} \tag{1}$$

where P_E represents the radiated power from the transmitting antenna, G_1 and G_2 are the antennas gains, G_R is the power gain of the reception front end (low noise amplifier and mixer), λ is the wavelength and d is the hertzian link length. A_s represents all the other losses that are not shown in Fig. 2 (lines, diplexers,…). The noise arriving at the demodulator consists of two contributions: the noise received by the antenna and the noise added by the reception front end. Both noises depend on the channel bandwidth (that can be considered as the noise bandwidth B_N) approximately equal to the symbol rate (for MAQ modulations).
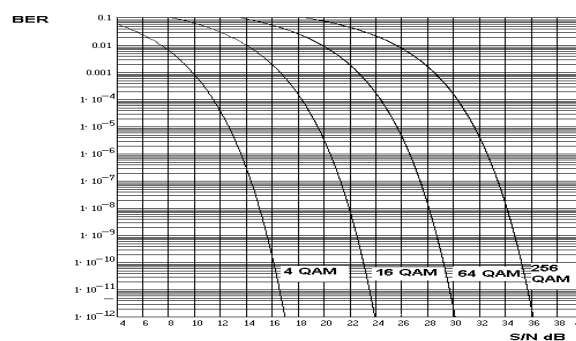
Fig. 1 Bit error rate as a function of the signal to noise ratio

The noise power at the reception (or antenna noise) is given by Eq. 2:

$$N_A = k T_A B_N \tag{2}$$

where k is the Boltzmann's constant and T_A the equivalent noise temperature of the antenna (equal to the room temperature for hertzian terrestrial links). The noise power added by the receiver depends upon its noise figure F. Seen from the receiver input, this power is given by Eq. 3.

$$N_a = k T_a B_N \tag{3}$$

where the equivalent noise temperature T_a corresponds to the noise added power (Eq. 4):
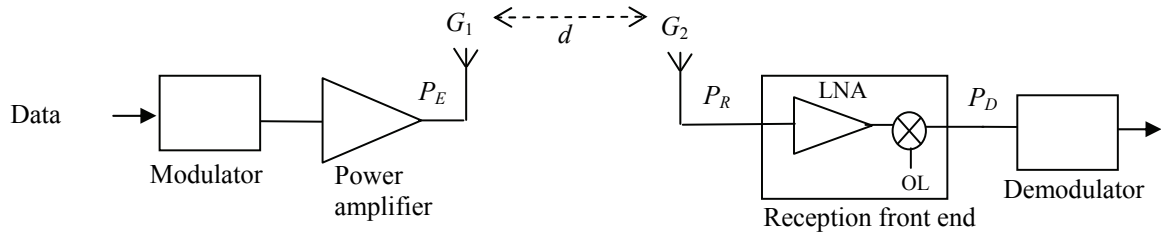
Fig. 2 Power balance for a hertzian link

$$F = 1 + \frac{T_a}{T_0} \quad (4)$$

T_0 is the reference temperature equal to 290 K. The carrier to noise ratio

$$C/N = \frac{P_E G_1 G_2 \left(\frac{\lambda}{4\pi d}\right)^2 \frac{1}{A_s}}{k T_0 F B_N} \quad (5)$$

This ratio is the same at the input of the demodulator because the receiver noise is seen from the input and then the receiver is considered as not noisy. For a given reception quality (i.e. a given value for C/N), if the receiver noise figure is most improved it is possible to reduce the transmitted power P_E in the same proportions. This is an important point for decreasing the radiofrequency transmitter power and hence for attenuating the electromagnetic pollution.

For a mobile phone uplink (from the user to the base station), the receiver noise figure improvement allows a significant decrease of the transmitted power from the cell phone and then the power sent to the user's brain. This is currently the far most important health hazard due to the radiofrequency waves. This is also true, but less significantly, for all the domestic radiofrequency devices (e.g. Wi-Fi). If the transmitted power decreases, the batteries must deliver less power. This increases the cell phone autonomy.

It is also possible, when the transmitted power is kept, to increase the distance between the transmitter and the receiver. A decrease of a factor 2 for the noise figure (3 dB) allows increase the distance by a factor 4. The cellular network mesh would be greatly lightened. This would be a great benefit for the electromagnetic environment, the batteries lifetime, the cost for the operators and the health for the users.

III. NOISE FIGURE FOR A TWO-PORT

A. Thermal Noise of a One-port

When a one-port is place at a temperature T, it supplies a noise spectral power density kT (k is the Boltzmann's constant equal to 1.381×10^{-23} J.K^{-1}). This means that the available power within a frequency band B_N is equal to kTB_N. The one-port can be represented as a Thévenin's

source whose impedance is $\underline{Z}_S$ and its available voltage is $\underline{e}_S$ given by its RMS value e_{Seff} (Eq. 6):

$$e_{Seff}^2 = 4kT\Delta f \, \text{Re}\left(\underline{Z}_S\right) \quad (6)$$

or as a Norton's source whose admittance is $\underline{Y}_S$ and its available current is $\underline{i}_S$ given by its RMS value i_{Seff} (Eq. 7):

$$i_{Seff}^2 = 4kT\Delta f \, \text{Re}\left(\underline{Y}_S\right) \quad (7)$$

B. Definition of a Two-port Noise Figure

The definition of the noise figure for a two-port (Eq. 8) is based upon the comparison between the signal to noise ratio at the input and output.

$$F = \frac{S_I/N_I}{S_O/N_O} \quad (8)$$

S_I is the power of the signal supplied by the source. S_O is the power of the signal that the two-port transmits to its load. N_O is the noise power that the two-port transmits to its load. N_I is the power that a passive one-port would supply to the two-port input. This two port would have the same Thévenin's impedance than the actual source and its noise temperature would be equal to $T_0 = 290$ K. This power is complicate to calculate because it depends upon the two-port input impedance and, hence, on the two-port load impedance. As far as the power refers to a temperature, it is easier to manipulate available powers. Moreover, the ratio between the actual power and the available power is the same for the signal and for the noise. This ratio simplifies and the noise figure may be calculated from available power as in Eq. 9.

$$F = \frac{S_{Iav}/N_{Iav}}{S_{Oav}/N_{Oav}} = \frac{N_{Oav}}{kT_0 B_N G_{av}} \quad (9)$$

where G_{av} is the two-port available power gain. The available gain at the output is the sum of the input noise amplified by the two-port and the two-port additional noise. In terms of available powers, this is written as in Eq. 10.

$$N_{Oav} = kT_0 B_N G_{av} + N_{addav} \quad (10)$$

Finally, the noise figure can be expressed as in Eq. 11.

$$F = 1 + \frac{N_{addav}}{kT_0 B_N G_{av}} \qquad (11)$$

C. Cascaded Two-ports

When two two-ports are cascaded, the output noise is:
- the source noise amplified by the two two-ports,
- the first two-port additional noise amplified by the second two-port,
- the second two-port additional noise.
- In terms of available noise powers (Eq. 12):

$$N_{Oav} = kT_0 \Delta f G_{av1} G_{av2} + N_{addav1} G_{av2} + N_{addav2} \qquad (12)$$

Using Eq. 9, The total noise figure F can be expressed as a function of the two-ports noise figures F_1 and F_2 and the available power gain of the first two-port G_{av1} (Eq. 13).

$$F = F_1 + \frac{F_2 - 1}{G_{av1}} \qquad (13)$$

This relation is known as the Friis formula [4].

D. Passive two-port

If a passive two-port whose temperature is T is supplied by a source at the same temperature the output available noise power is kTB_N. Considering Eq. 10:

$$N_{Oav} = kTB_N = kTB_N G_{av} + N_{addav} \qquad (14)$$

If it is introduced in Eq. 11:

$$F = \frac{T}{T_0}\left(\frac{1}{G_{av}} - 1\right) + 1 \qquad (15)$$

E. Variation of the Noise Figure with the Source Admittance

The noise figure is simply expressed with the available powers. So, it is natural that it depends on the source impedance or admittance ($\underline{Y_S} = G_S + jB_S$) and that it does not on the load impedance. The variation of the noise figure is given in Eq. 16.

$$F = F_{MIN} + \frac{R_n}{G_S}\left|\underline{Y_S} - \underline{Y_{OPT}}\right|^2 \qquad (16)$$

In Eq. 16, four independent parameters appear:
- the real and imaginary parts of $\underline{Y_{OPT}}$ which is the source admittance that corresponds to the minimum noise figure,
- F_{MIN} which is the minimum noise figure,
- R_N, called the noise resistance, which corresponds to the variation strength when $\underline{Y_S}$ becomes different from $\underline{Y_{OPT}}$.

The variation of F against the reflection coefficient $\underline{\Gamma_S}$ corresponding to $\underline{Y_S}$ is shown in Fig. 3.
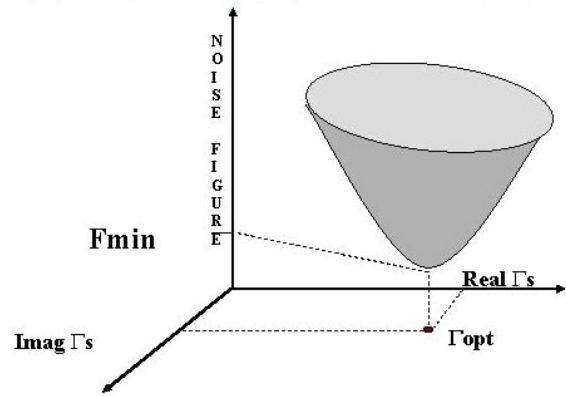
Fig. 3 Variation of the noise figure v.s. the source reflection coefficient

The circuit designer's know-how consists of having the optimum impedance for the noise figure and for the power transfer coincide [5]. An example of solution is shown in Fig. 4. An impedance placed in the transistor emitter allows to have $\underline{Z_{OPT}}$ and $\underline{Z_{in}}$ conjugate to each other. Then, matching input and output two-ports are placed in order to have a maximum gain and hence a minimum noise figure.
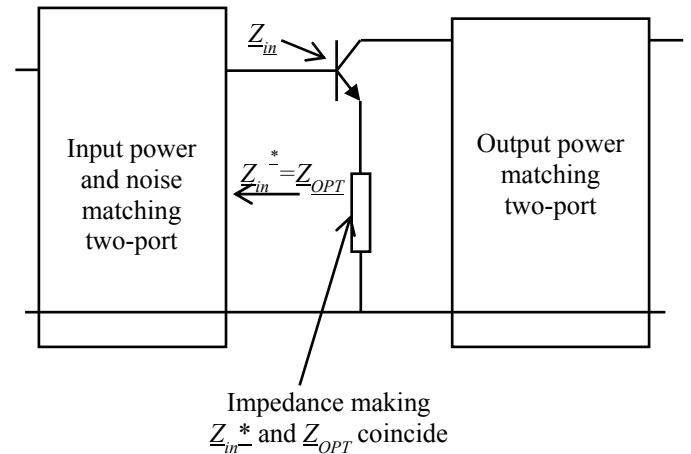
Fig. 4 Example of low noise amplifier design principle

IV. NOISE FIGURE MEASUREMENT

A. Measurement Principle

When a one-port placed at the input of a two-port is at two temperature T_1 and T_2 (and if its Thévenin's impedance has not changed), the available output powers are given in Eq. 17.

$$\begin{cases} N_{Oav1} = G_{av}kB_N T_1 + N_{addav} \\ N_{Oav2} = G_{av}kB_N T_2 + N_{addav} \end{cases} \qquad (17)$$

The one-port is generally a noise source. T_1 is often the room temperature. T_2, called hot temperature, is given by

the noise source manufacturer by its excess noise ratio (ENR) which is periodically calibrated. For any temperature, the excess noise ratio is given by Eq. 18.

$$R = \frac{T}{T_0} - 1 \qquad (18)$$

Eq. 17 can be considered as a set of two equations with two unknown $G_{av}kB_N$ and N_{addav}. The ratio between the two measured powers is the same for the available powers (Eq. 19).

$$Y = \frac{N_{Oav2}}{N_{Oav1}} = \frac{N_{O2}}{N_{O1}} \qquad (19)$$

When the solution is put into Eq. 11, the noise figure is:

$$F = \frac{R_2 - YR_1}{Y - 1} \qquad (20)$$

The noise source calibration gives the ENR as $10\log(R_2)$. A usual value for the ENR is 15 dB (9461 K) that corresponds to an equivalent noise temperature and not to a physical one.

B. Ideal Measurement Setup

An ideal measurement setup is shown in Fig. 4. The isolator placed in the noise one-port makes the source impedance independent on the noise source temperature. The isolator placed in the noise figure meter allows consider it as a unilateral two-port. The noise source, the isolator and the connections constitute the noise one-port. The temperature T_2 must be corrected by the elements losses. The second isolator, the mixer the amplifier and the receiver constitute the noise figure meter (NFM). Fig. 5 shows a simplified diagram of the setup.

If we suppose that the noise one-port impedance is independent on the temperature, the noise figure F of the set DUT-NFM is given by Eq. 20 where N_{O1} and N_{O2} are the measured values for each temperature. In order to know the NFM noise figure, we must perform a calibration as shown in Fig. 6.
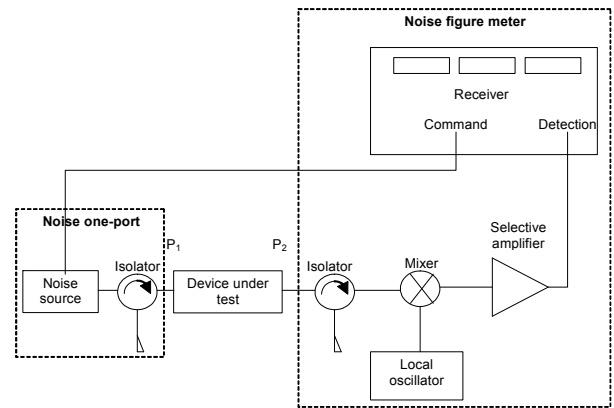
Fig. 4 Ideal setup for noise figure measurement
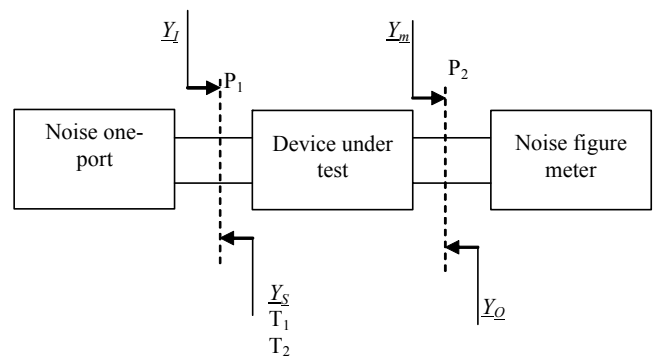
Fig. 5 Simplified diagram of the setup in Fig. 4
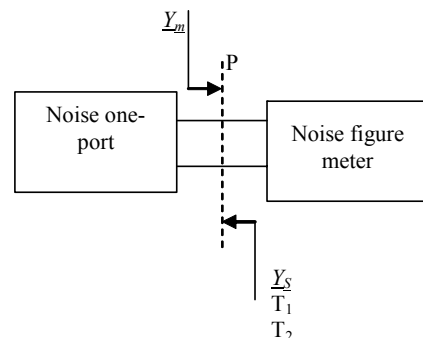
Fig. 6 Calibration of the NFM

The measured noise powers are N'_{O1} and N'_{O2}. The calculated noise figure F_m corresponds to the source admittance Y_S. If Y_O and YS are equal, i.e. when the source admittance is equal to the DUT output iterative admittance, the Friis formula (Eq. 13), can be used to calculate the DUT noise figure F_X.

$$F_X = F - \frac{F_m - 1}{G_{avX}} \qquad (21)$$

We must know the DUT available power gain G_{avX}. When the source admittance is equal to the output iterative admittance, the available power gain G_{avX} is equal to the insertion gain Gi_{nsX}. It can be calculated from the measured

powers with the DUT N_{O1} and N_{O2} and without the DUT N'_{O1} and N'_{O2}.

$$G_{insX} = \frac{N_{O2} - N_{O1}}{N'_{O2} - N'_{O1}} \qquad (22)$$

Hence, we know all the necessary data to calculate F_X. It is very important to notice that:

- the noise source impedance must not depend on the temperature,
- the DUT must be close at its input by its output iterative impedance,
- the temperatures T_1 and T_2 must be known in the input plane of the DUT.

It is important to notice that we do not need the DUT electrical characteristics (S-parameters, Y-parameters,…).

Many commercial noise figure meters work in these conditions. The iterative impedance is supposed to be 50 Ω and the meters display the frequency, the insertion gain and the noise figure. The displayed noise figure is wrong if the conditions above are not fulfilled.

C. Classical Noise Parameters Measurement

The classical noise parameters measurement consists of placing several impedances in order to have at least 4 equations [6, 7]. The choice of the impedances must follow the rules below:

- the corresponding points on the Smith chart must not be placed on the same centered circle nor on the same chart diameter,
- the DUT must be stable for any frequency, even out of the studied bandwidth,
- the corresponding point of the DUT output impedance must be kept inside the Smith chart.

We could expect that only 4 impedances are necessary. Due to the measurement uncertainty, a large number of impedances is used. The noise parameters are then obtained by numerical optimization of the Friis formula (Eq. 11) [8, 9].

The setup is described in Fig. 7. A vector network analyzer is calibrated between planes P1 and P2 in order to measure the DUT S-parameters and the different impedances shown at the DUT input. If three standards are put in plane P3, it is possible to know the corrected temperature in plane P1. A low noise amplifier (LNA) is put as close as possible to the switch to minimize the setup noise figure.
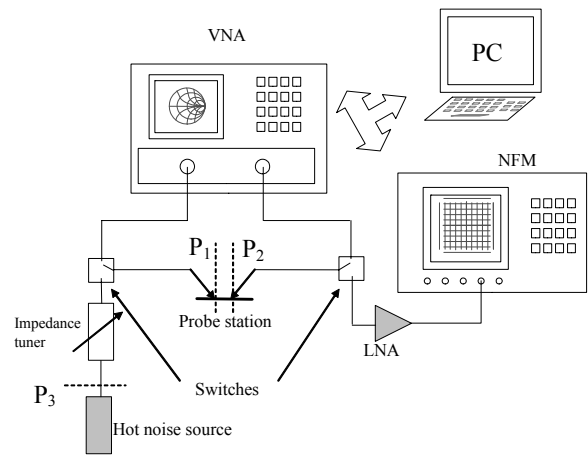
Fig. 7 Noise parameters setup using the multi-impedance method

V. NOISE PARAMETERS MEASUREMENT USING THE POWER WAVES FORMALISM

A. Impedance Correlation Matrix

A noisy two-port can be represented by a non-noisy two port with two correlated noise voltages as in Fig. 8 [10, 11].
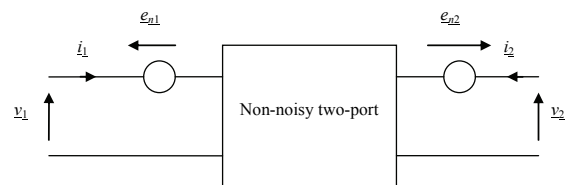
Fig. 8 Noisy two-port in impedance representation

This can be written by a matrix relation:

$$\begin{pmatrix} \underline{v_1} \\ \underline{v_2} \end{pmatrix} = \begin{pmatrix} \underline{Z_{11}} & \underline{Z_{12}} \\ \underline{Z_{21}} & \underline{Z_{22}} \end{pmatrix} \begin{pmatrix} \underline{i_1} \\ \underline{i_2} \end{pmatrix} + \begin{pmatrix} \underline{e_{n1}} \\ \underline{e_{n2}} \end{pmatrix} \qquad (23)$$

We define a correlation matrix by Eq. 24:

$$\underline{\mathbf{C_z}} = \begin{pmatrix} \underline{C_{Z11}} & \underline{C_{Z12}} \\ \underline{C_{Z21}} & \underline{C_{Z22}} \end{pmatrix} = \frac{1}{B_N} \begin{pmatrix} \langle \underline{e_{n1}} \cdot \underline{e_{n1}}^* \rangle & \langle \underline{e_{n1}} \cdot \underline{e_{n2}}^* \rangle \\ \langle \underline{e_{n2}} \cdot \underline{e_{n1}}^* \rangle & \langle \underline{e_{n2}} \cdot \underline{e_{n2}}^* \rangle \end{pmatrix} \qquad (24)$$

B. S-parameter Correlation Matrix

We can also represent the noisy two-port by its scattering parameters representation in Eq. 25.

$$\begin{pmatrix} \underline{b_1} \\ \underline{b_2} \end{pmatrix} = (\underline{\mathbf{S}}) \begin{pmatrix} \underline{a_1} \\ \underline{a_2} \end{pmatrix} + \begin{pmatrix} \underline{b_{n1}} \\ \underline{b_{n2}} \end{pmatrix} \qquad (25)$$

which corresponds to the flow chart in Fig. 9.
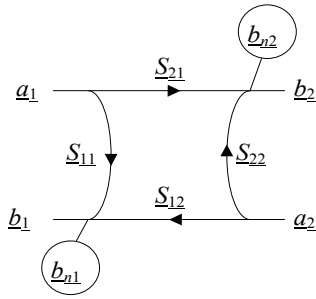
Fig. 9 Flow chart of the representation of a two-port by its scattering parameters

The terms $\underline{a_1}$, $\underline{b_1}$, $\underline{a_2}$, $\underline{b_2}$, $\underline{b_{n1}}$, and $\underline{b_{n2}}$ are complex and expressed in $W^{1/2}$. The noise sources $\underline{b_{n1}}$ and $\underline{b_{n2}}$ are correlated. The correlation matrix is defined as in Eq. 26.

$$\left(\underline{\mathbf{C_S}}\right) = \frac{1}{B_N}\begin{pmatrix} \langle\underline{b_{n1}}\cdot\underline{b_{n1}^*}\rangle & \langle\underline{b_{n1}}\cdot\underline{b_{n2}^*}\rangle \\ \langle\underline{b_{n2}}\cdot\underline{b_{n1}^*}\rangle & \langle\underline{b_{n2}}\cdot\underline{b_{n2}^*}\rangle \end{pmatrix} \quad (26)$$

The notation $<\underline{a}.\underline{b}^*>$ means the correlation between $\underline{a}$ and $\underline{b}$. The matrix $\underline{\mathbf{C_S}}$ elements consist of four parameters expressed in $W.Hz^{-1}$, two real self-correlations and the real and imaginary parts of the intercorrelation. They are related to the 4 conventional noise parameters.

C. Calibration of the setup

During the calibration process the device under test between planes P_1 and P_2 is replaced by a thru. The flow chart is given in Fig. 10 [12].
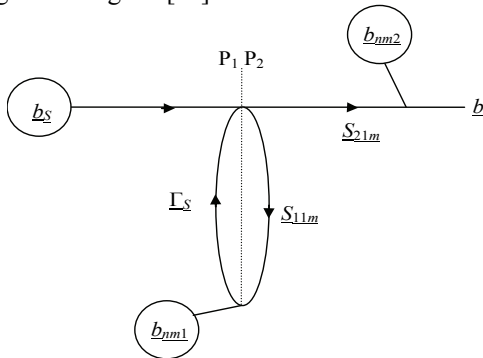
Fig. 10 Flow chart of the calibration

$\underline{b_S}$ and $\underline{\Gamma_S}$ are the noise wave and the reflection coefficient of the source seen from plane P_1. Five measurements are done with five different sources: a hot noise source with a known excess noise ratio (i=1), a short (i=2), an open (i=3), a shorted 3 dB attenuator (i=4) and an open 3 dB attenuator (i=5). The measured noise powers $N_i=<\underline{b_i}.\underline{b_i}^*>$ are linearly related to the set-up characteristics by Eq. 27 and 28.

$$\begin{pmatrix} N_1 \\ N_2 \\ N_3 \\ N_4 \\ N_5 \end{pmatrix} = \left(\mathbf{M}_m\right)\begin{pmatrix} kB_N\left|S_{21m}\right|^2 \\ \langle\underline{b_{nm1}}.\underline{b_{nm1}^*}\rangle\left|S_{21m}\right|^2 \\ \langle\underline{b_{nm2}}.\underline{b_{nm2}^*}\rangle \\ \mathrm{Re}\left(\langle\underline{b_{nm1}}.\underline{b_{nm2}^*}\rangle S_{21m}\right) \\ \mathrm{Im}\left(\langle\underline{b_{nm1}}.\underline{b_{nm2}^*}\rangle S_{21m}\right) \end{pmatrix} = \left(\mathbf{M}_m\right)\begin{pmatrix} X_1 \\ X_2 \\ X_3 \\ X_4 \\ X_5 \end{pmatrix} \quad (27)$$

with

$$\begin{cases} M_{m1j} = T_j\dfrac{1-\left|\Gamma_j\right|^2}{\left|1-\underline{S_{11m}}\underline{\Gamma_j}\right|^2} \\[4mm] M_{m2j} = \dfrac{\left|\Gamma_j\right|^2}{\left|1-\underline{S_{11m}}\underline{\Gamma_j}\right|^2} \\[4mm] M_{m3j} = 1 \\[4mm] M_{m4j} = 2\,\mathrm{Re}\left(\dfrac{\Gamma_j}{1-\underline{S_{11m}}\underline{\Gamma_j}}\right) \\[4mm] M_{m5j} = -2\,\mathrm{Im}\left(\dfrac{\Gamma_j}{1-\underline{S_{11m}}\underline{\Gamma_j}}\right) \end{cases} \quad (28)$$

In this matrix, T_1 is the corrected hot temperature in plane P_1 and T_2 to T_5 are the room temperature. T_1 can be calculated from the noise source ENR and the S-parameters of the two-port situated between P_3 and P_1. They can be known with an SOL (short-open-load) process with $\underline{\Gamma_1}$, $\underline{\Gamma_2}$ and $\underline{\Gamma_3}$. The reference impedance in plane P_3 is the hot noise source impedance that must theoretically be real and may be different from 50 Ω. The values for X_1, X_2, X_3, X_4 and X_5 are obtained in inversing Eq. 27.

D. DUT measurement

The total flow chart with the DUT is shown in Fig. 11.
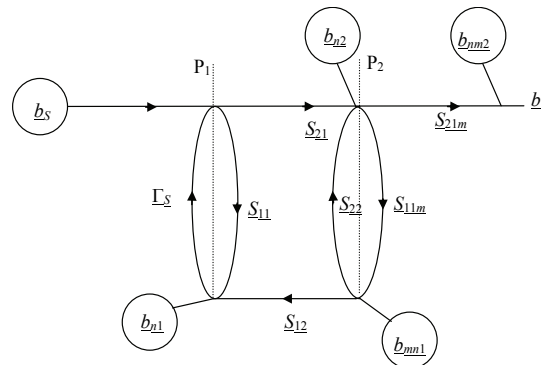
Fig. 11 Flow chart of the set-up with the DUT

The DUT S-parameters are measured with the VNA. The measured noise power is N_i for each of the four impedances placed in plane P_3: i.e. a short, an open, a shorted attenuator

and an open attenuator. We define an intermediary normalized noise power by Eq. 29.

$$n_i = \frac{N_i|\underline{D}|^2}{X_1 T_0} - \frac{T_2}{T_0}\left(1 - |\underline{\Gamma}_i|^2\right) - \frac{X_2}{X_1 T_0}\left|S_{22} - \underline{\Gamma}_i \Delta \underline{S}\right|^2$$
$$+ \frac{X_3|\underline{D}|^2}{X_1 T_0} - 2\operatorname{Re}\left(\frac{X_4 + jX_5}{X_1 T_0}\left(\underline{S_{22}} - \underline{\Gamma}_i \Delta S\right)\underline{D}^*\right) \quad (29)$$

with

$$\underline{D} = 1 - \underline{\Gamma}_i \underline{S_{11}} - \underline{S_{22}}\underline{S_{11m}} + \underline{\Gamma}_i \underline{S_{11m}}\Delta \underline{S} \quad (30)$$

and

$$\Delta \underline{S} = \underline{S_{11}}\underline{S_{22}} - \underline{S_{12}}\underline{S_{21}} \quad (31)$$

This normalized power linearly depends on the DUT correlation matrix $\underline{\mathbf{C_S}}$.

$$\begin{pmatrix} n_1 \\ n_2 \\ n_3 \\ n_4 \end{pmatrix} = \frac{1}{kT_0}(\mathbf{M})\begin{pmatrix} C_{S11} \\ C_{S22} \\ \operatorname{Re}\left(\underline{C_{S12}}\right) \\ \operatorname{Im}\left(\underline{C_{S12}}\right) \end{pmatrix} \quad (32)$$

With:

$$\begin{cases} M_{1j} = |\underline{\Gamma}_j|^2|\underline{S_{21}}|^2 \\ M_{2j} = |1 - \underline{S_{11}}\underline{\Gamma}_j|^2 \\ M_{3j} = 2\operatorname{Re}\left(\underline{\Gamma}_j \underline{S_{21}}\left(1 - \underline{S_{11}}^*\underline{\Gamma}_j^*\right)\right) \\ M_{4j} = -2\operatorname{Im}\left(\underline{\Gamma}_j \underline{S_{21}}\left(1 - \underline{S_{11}}^*\underline{\Gamma}_j^*\right)\right) \end{cases} \quad (33)$$

The values for C_{S11}, $\underline{C_{S12}}$ and C_{S22} are obtained in inversing Eq. 32. The conventional noise parameters F_{MIN}, R_N and $\underline{\Gamma}_{OPT}$ can be calculated from these parameters.

VI. SOME RESULTS OF THIS METHOD

A. Passive Two-port

To validate our method we choose a passive component for which the noise parameters are exactly known from his S parameters. The DUT consists of an inductor in an SiGe technology. The measurements have been made between 1 GHz and 7 GHz and the previous calibration results have been used.

Fig. 12 shows the extracted conventional noise parameter F_{MIN} compared to their calculated values from S parameters:

$$\left(\mathbf{C_S}\right) = kT\left((\mathbf{I}) - (\underline{\mathbf{S}})(\underline{\mathbf{S}})^\dagger\right) \quad (34)$$

Where superscript † indicates the transposed-conjugate.
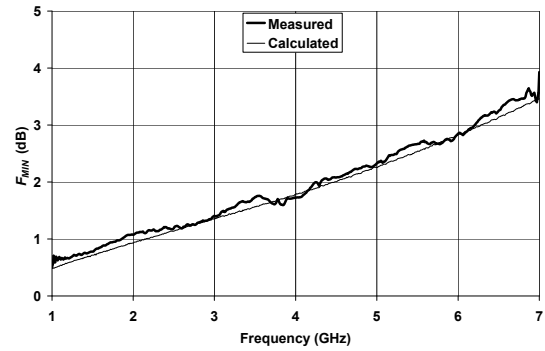
Fig. 12 Measured and calculated F_{MIN} for a passive two-port

B. Noise Model of a Bipolar Transistor

The model for the transistor that we have used is shown in Fig. 13 [13].
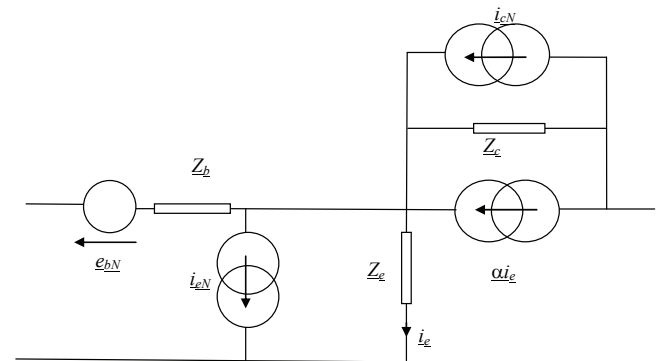
Fig. 13 Extrinsic model for a bipolar transistor

The elements of this model may be easily extracted from the electrical impedance matrix $\underline{\mathbf{Z}}$:

$$\begin{cases} \underline{Z_b} = \underline{Z_{11}} - \underline{Z_{12}} \\ \underline{Z_c} = \underline{Z_{22}} - \underline{Z_{21}} \\ \underline{\alpha} = \dfrac{\underline{Z_{12}} - \underline{Z_{21}}}{\underline{Z_{22}} - \underline{Z_{21}}} \\ \underline{Z_e} = \underline{Z_{12}} \end{cases} \quad (35)$$

and the correlation matrix $\underline{\mathbf{Cz}}$.

$$\begin{cases} C_{Z11} = 4kT\operatorname{Re}\left(\underline{Z_b}\right) + |\underline{Z_e}|^2\left\langle i_{eN} \cdot i_{eN}^*\right\rangle \\ \underline{C_{Z12}} = \underline{Z_c}\underline{Z_{21}}^*\left\langle i_{eN} \cdot i_{eN}^*\right\rangle + \underline{Z_e}\underline{Z_c}^*\left\langle i_{eN} \cdot i_{cN}^*\right\rangle \\ C_{Z22} = |\underline{Z_{21}}|^2\left\langle i_{eN} \cdot i_{eN}^2\right\rangle + |\underline{Z_c}|^2\left\langle i_{cN} \cdot i_{cN}^*\right\rangle \\ \quad + 2\operatorname{Re}\left(\underline{Z_{21}}\underline{Z_c}^*\left\langle i_{eN} \cdot i_{cN}^*\right\rangle\right) \end{cases} \quad (36)$$
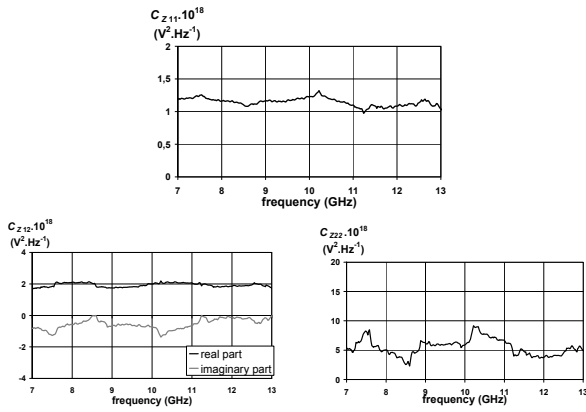
Fig. 14 Measured correlation matrix elements

The noise current RMS values and their correlation coefficient have been extracted and shown in Fig. 15.

$$\underline{C} = \frac{\left\langle \underline{i}_{eN} \cdot \underline{i}_{cN}^{\;*} \right\rangle}{\sqrt{\left\langle \underline{i}_{eN} \cdot \underline{i}_{eN}^{\;*} \right\rangle \left\langle \underline{i}_{cN} \cdot \underline{i}_{cN}^{\;*} \right\rangle}} \tag{37}$$
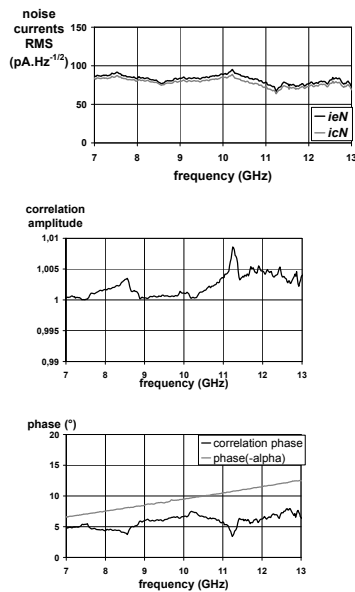
Fig. 15 Noise currents and their correlation coefficient

The current sources have almost the same RMS value. This corresponds to some results in the literature. But this value (between 70 and 90 pA.Hz$^{-1/2}$) is far higher than the value which results from the shot noise (40 pA.Hz$^{-1/2}$). This is due to the simplicity of the model in Fig. 13. In particular, $\underline{Z}_e$ can be split into two parts, one corresponding to the emitter-base junction and the other to the access. They can be separated by the extraction for several emitter DC currents. The effect of the lossy substrate can also explain this difference. The magnitude of the correlation coefficient is equal to unity and its phase is close to the

phase of $\underline{\alpha}^*$. These results are also found in the literature.

From this model, the conventional noise parameters as shown are calculated. Fig. 16 compares the optimal reflection coefficient $\underline{\Gamma}_{OPT}$ related to $\underline{Y}_{OPT}$ to the conjugate of the transistor input reflection coefficient $\underline{S}_{11}^*$. This parameter corresponds to the maximum power transfer between the source and the component. All the know-how of the designer consists of adding elements in order to have $\underline{\Gamma}_{OPT}$ and $\underline{S}_{11}^*$ coincide. Then, he must add an adaptation two-port between the source and the component in order to reach an equivalent source impedance related to $\underline{S}_{11}^*$.
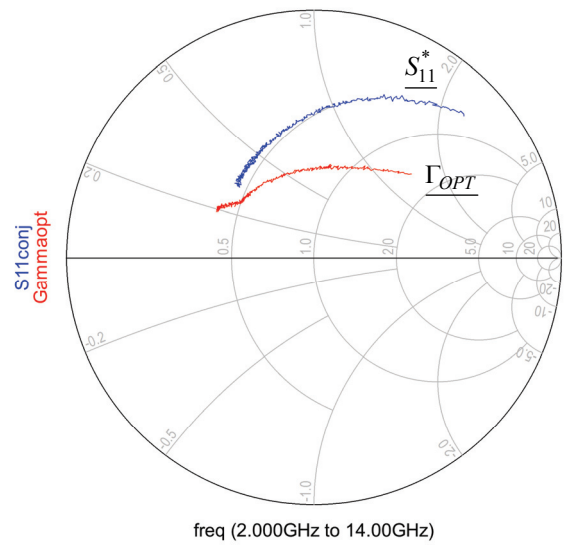
Fig. 16 Measured $\underline{S}_{11}{}^*$ and $\underline{\Gamma}_{OPT}$ for a heterojunction bipolar transistor

VII. MEASUREMENT METHOD WITHOUT A HOT SOURCE

Modern network analyzers can measure a noise power level. Some are able to measure a noise figure. We propose to use a modern network analyzer (an Agilent PNA-X) to measure the four noise parameters of a two-port. In this paper, we only describe the calibration of the receiver gain. The other calibration parameters are determined by a more conventional method.

Many calibration methods exist for the network analyzer calibration. One of the most known is the SOLT (short-open-load-thru) method. The model consists of 5 terms (the cross-talk is neglected) for the forward measurement and 5 other terms for the reverse measurement. They are described by the flow chart in Fig. 17 for forward measurement.
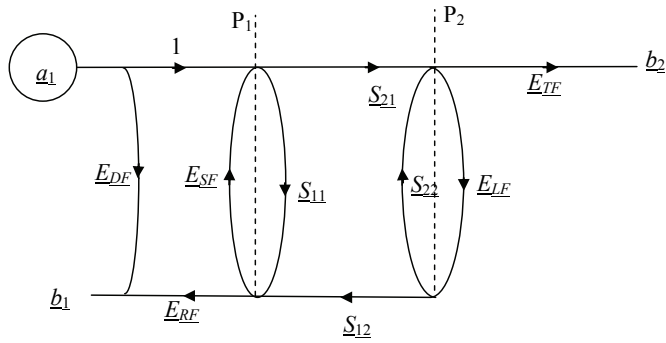
Fig. 17. Flow chart of the SOLT

If we compare Fig. 11 and Fig. 17, the receiver input reflection coefficient S_{11m} and the load mismatch E_{SF} are the same [15]. It is suggested that the receiver gain S_{21m} and the tracking term E_{TF} are similar. Usually, $kB_N|S_{21m}|^2$ is determined by noise measurements with the hot noise source and E_{TF} is simply deducted from power level ratios. So, if we know B_N, which must be measured separately, the noise source is no longer useful. The setup becomes far easier as in Fig. 18.
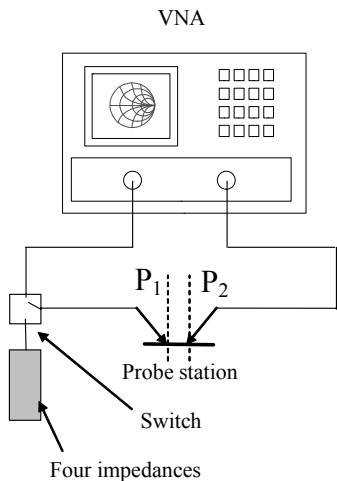
Fig. 18 Setup without hot source

Eq. 27 becomes Eq. 38:

$$\begin{pmatrix} N_2 \\ N_3 \\ N_4 \\ N_5 \end{pmatrix} = (\mathbf{M}_m) \begin{pmatrix} \langle \underline{b}_{nm1}.\underline{b}^*_{nm1} \rangle |\underline{S}_{21m}|^2 \\ \langle \underline{b}_{nm2}.\underline{b}^*_{nm2} \rangle \\ \mathrm{Re}\left(\langle \underline{b}_{nm1}.\underline{b}^*_{nm2} \rangle \underline{S}_{21m}\right) \\ \mathrm{Im}\left(\langle \underline{b}_{nm1}.\underline{b}^*_{nm2} \rangle \underline{S}_{21m}\right) \end{pmatrix} = (\mathbf{M}_m) \begin{pmatrix} X_2 \\ X_3 \\ X_4 \\ X_5 \end{pmatrix}$$

(38)

And X_1 is calculated separately.

$$X_1 = kB_N |\underline{E}_{TF}|^2$$

(39)

The rest of the process is the same. A first approach has

been made with a simple VNA (an Agilent E5071C) just to check the order of magnitude. Fig. 19 compares $|S_{21m}|$ and $|E_{TF}|$. The orders of magnitude are the same, but further measurement with a more sensitive VNA is needed and will be presented at the conference.
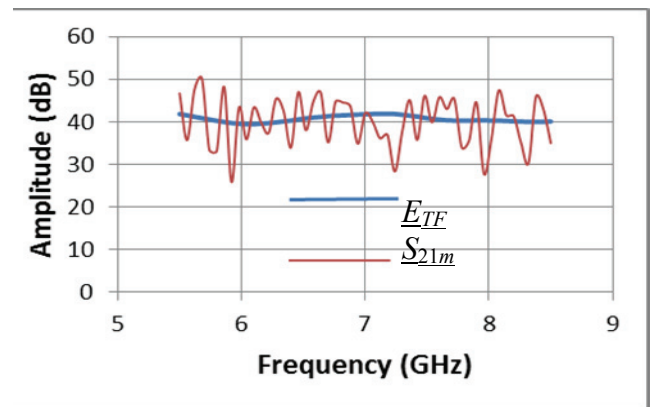
Fig. 19 Comparison between $|S_{21m}|$ measured with a hot source and the $|E_{TF}|$ term of the VNA error model.

VIII. CONCLUSION

The noise characteristics of RF devices are very important for the base stations mesh scaling and the mobile stations sensitivity. If these characteristics are efficient, the number of stations can be lowered. If the receivers sensitivity is low, less power is requested and less power is transmitted into the user's brain.

The accurate knowledge of the noise characteristics of components is necessary for the devices design. Usually, the four noise parameters R_N, F_{MIN}, G_{OPT} and B_{OPT} are measured after a numerical optimization of non-linear equations. The new method that we propose uses auxiliary data that are linearly dependent on the correlation matrix elements. So, the noise parameters calculation is simpler and faster.

The use of the correlation matrix is also useful to deal with component noise modeling. We have shown an example of an HBT using the impedance correlation matrix.

The new vector network analyzers may measure the noise power. In particular, the measurement bandwidth can be chosen, even if it must be separately measured. This allows to measure the four noise parameters (in terms of S-correlation matrix elements) without a hot noise source. Hence, a specific noise figure meter and a noise source are no longer necessary. It will be no longer necessary to send le noise source every year for calibration.

The main problem is that during the VNA calibration procedure, the input level at Port 2 may be too high, eventually higher than the authorized maximum level, due to the high S_{21m} gain. The use of a composite receiver between the plane P2 and the VNA port 2 can partially solve this problem [16]. But it makes impossible the measurement of the S_{12} and S_{22} DUT parameters without disconnection.

REFERENCES

[1] D. Pasquet, F. Temcamani, "Contribution of the Noise Parameters Knowledge to Energy Saving and RF Radiation Decrease", *16th IEEE Mediterranean Electrotechnical Conference, MELECON 2012*, Yasmine-Hammamet, Tunisia, March 25-28, 2012.

[2] Hikmet SARI, "Transmission des Signaux Numériques", *Techniques de l'Ingénieur*, Reference E7100, 10 juin 1995.

[3] A. Goldsmith, *Wireless Communications*, Cambridge University Press, 2005.

[4] H.T. Friis, "Noise Figures of Radio Receivers", *Proceedings of the IRE*, vol. 32, issue 7, Nov. 1944, pp. 419-422.

[5] I. Bahl, *Fundamentals of RF and Microwave Transistor Amplifiers*, Wiley, 2009.

[6] R.Q. Lane, "The Determination of Noise Parameters", *Proc. IEEE*, vol. 57, issue 8, pp. 1461-1462, Aug. 1969.

[7] M. Mitama, H. Katoh, "An Improved Computational Method for Noise Parameter Measurement", *IEEE Trans. on Microwave Theory and Technique*, vol. 27, issue 6, June 1979, pp. 612-615.

[8] L. Escotte, R. Plana, J. Graffeuil, "Evaluation of Noise Parameter Extraction Methods", *Trans. on Microwave Theory and Technique*, vol. 41, issue 3, March 1993, pp. 382-387.

[9] A. Boudiaf, M. Laporte, J. Dangla, G. Vernet, "Accuracy Improvements in Two-Port Noise Parameter Extraction Method", *IEEE International Microwave Symposium Digest*, Albuquerque, NM, USA, June 1992, pp. 1569-1572.

[10] H. Rothe, W. Dahlke, "Theory of Noisy Fourpoles", *Proceedings of the IRE*, vol. 56, no. 6, June 1956, pp. 811-818.

[11] H. Hillebrand, P. Russer, "An Efficient Method for Computer Aided Noise Analysis of Linear Amplifier Networks", *IEEE Trans. on Circuits and Systems*, vol. 23, no. 4, Apr. 1976, pp. 235-238.

[12] D. Pasquet, E. Bourdel, S. Quintanel, T. Ravalet, P. Houssin, "New Method for Noise-Parameter Measurement of a Mismatched Two-Port", *IEEE Trans. on Microwave Theory and Technique*, vol. 56, no. 9, Sept. 2008, pp. 2136-2142.

[13] M. Rudolph, R. Doerner, L. Klapproth, P. Heymann, "An HBT Noise Model Valid up to Transit Frequency", *IEEE Electron Devices Letters*, vol. 20, no. 1, Jan. 1999, pp. 24-26.

[14] M. Rudolph, R. Doerner, P. Heymann, "Direct Extraction of HBT Equivalent-Circuit Elements", *IEEE Trans. On Microwave Theory and Technique*, vol. 47, no. 1, Jan. 1999, pp. 82-84.

[15] D. Pasquet, Z. Huang, C. Qiu, D. Lesénéchal, P. Descamps, "Calibration for Noise Parameters Measurement with a VNA and witout a Noise Source", *81th ARFTG Microwave Measurement Conference*, Seattle June 7, 2013.

[16] Anritsu Application Note, "*Noise Figure Measurements, VectorStar, Making Successful, Confident NF Measurements on Amplifiers*", AP # 11410-00637A, June 2012.